Prediction of Combustion in Homogeneous-Charge Spark-Ignition Engines

H.G.Weller, S.Uslu, A.D.Gosman, R.R.Maly*, R.Herweg* and B.Heel*

Mechanical Engineering Department
Imperial College
Exhibition Road, London SW7 2BX
England
* *Daimler-Benz AG*

ABSTRACT

A new modelling approach for premixed combustion in spark-ignition engines based on detailed analysis of the interaction of the thin flame with the turbulent flow field is presented and compared with experimental data obtained in a special research engine, using advanced laser diagnostics. The new model is shown to correctly predict the qualitative and quantitative behaviour of the flame, in contrast to many previous approaches which assume that the combustion rate is linked in a simple fashion with the turbulence time or length scales.

INTRODUCTION

Background. Over the past two decades much effort has been devoted to the development of multidimensional prediction methods for flow, heat transfer and combustion in reciprocating engines. The core components of the methods which determine their applicability and accuracy comprise the conservation equations governing the physical processes and numerical procedures for solving them in engine circumstances. On the numerical side substantial progress has been made and this, coupled with the rapid advances in computer technology, is causing the focus increasingly to shift onto the physics modelling, particularly of turbulence and combustion. Here progress has been slower in both areas, but especially the latter. Since turbulence modelling is a major topic in its own right, all that will be said about it here is that although current models are undoubtedly imperfect, they are probably not the limiting factor in combustion calculations: rather it is the combustion models themselves. These comments apply to both the 'conventional' ensemble-average analysis framework and the emerging 'large-eddy simulation' (LES) approach, since even for this the small length and time scales of combustion dictate that much of the physics is sub-grid and must therefore be modelled.

The homogeneous-charge engine presents, in principle, the fewest challenges to combustion analysis as compared with other types, where mixing effects on local stoichiometry and consequential burning rates must also be considered. Nevertheless, even for this 'simple' case there are no well-proven combustion models available, although many attempts have been made to develop them.

The most widely-used turbulent premixed combustion models can be broadly classified into three main categories (excluding the now-discredited practice of evaluating local reaction rates directly from chemical-kinetic expressions, taking no account of turbulent interactions), which will be loosely labelled, in order of chronological appearance, as 'eddy break up' (EBU), 'thin wrinkled flame' (TWF) and 'flame area evolution'(FAE).

In the EBU class, widely used for engine calculations (eg 1-3) little explicit account is taken of the flame structure and its interaction with the turbulence: rather the local burning rate is simply assumed to be controlled by small-scale 'turbulent mixing' with a characteristic time scale related to the turbulence dissipation scale. As discussed later, the latter assumption is incorrect.

TWF models (4-6), as the name implies, take recognition of some important aspects of the flame structure, namely that it is normally thin (of the order of the Kolmogorov scale) and wrinkled, the increased area being responsible for the increased burning rate over a smooth flame. Moreover most TWF models also assume that the flame locally burns in a laminar, one-dimensional mode (the so-called 'laminar flamelet' assumption) which has the important advantage of allowing detailed chemistry and flame-straining effects to be included in an economical way. Unfortunately these models also suppose that the characteristic scale of wrinkling can be linked in a simple way (typically proportional) to characteristic turbulence scales, which turns out, in engine circumstances, to be a weakness analagous to that of the EBU models: however this is not generally recognised presumably because there have been few applications.

The more recently-developed FAE models share some elements of the TWF class, notably the thin-flame assumption and in most, but not all cases, the presumption of laminar-flamelet burning. They differ however in the important respect that the local wrinkled flame area is obtained via a differential evolution equation for this or a related quantity; and the evolution equation allows for the fact that the area is influenced not only by the turbulence field, but also by the flame itself and by non-local effects. This approach, as has been shown in recent studies (7-10) and will also be demonstrated here, is able, in some instances, to provide more realistic engine predictions than the earlier methods.

Present Study. This paper is primarily concerned with the presentation and evaluation of a new model of premixed turbulent combustion which falls within the FAE category, but has some novel features as compared with others in this class. A (necessarily) brief outline of the model is presented in the next section, along with comments on the origins of the deficiencies of EBU and TWF models for engine applications. Following this, we describe the validation study, which involved gathering experimental data in a novel square-piston engine offering good optical access for advance laser diagnostics, including planar laser-induced fluorescence and Mie scattering measurements of the mixture and flame structures and particle laser velocimetry measurements of the flow field. These data are compared with predictions obtained using the STAR-CD multidimensional code, with the new combustion modelling embodied.

COMBUSTION MODELLING

Existing Models. A full mathematical model of turbulent combustion comprises conservation equations for mass, momentum, energy, turbulent transport and chemical species. Here we concentrate on the last-named, for it reflects the modelling assumptions regarding the flow/flame interactions of main interest here. Conventionally, a combination of ensemble and density-weighted averaging is applied to the instantaneous equations to produce

$$\frac{\partial \bar{\rho}\tilde{c}}{\partial t} + \nabla.\bar{\rho}\tilde{U}\tilde{c} - \nabla.(\bar{\rho}\,\tilde{D}_c\,\nabla\tilde{c}) = \tilde{w} \qquad (1)$$

where c is a non-dimensional species concentration or 'progress variable', defined to have limits unity and zero in the fully-burned and unburned states respectively, $\tilde{D}_c$ is a turbulent diffusion coefficient and $\tilde{w}$ is the reaction rate. The overbar (−) and tilda overbar (~) denote ensemble and density/ensemble averaging respectively.

The mean reaction rate $\tilde{w}$ is, within the original EBU framework, typically given by an expression of the form

$$\tilde{w} = A\, f(\tilde{c}) / \tilde{\tau}_c \qquad (2)$$

where A is an empirical coefficient, $f(\tilde{c})$ is an algebraic function of $\tilde{c}$ and τ_c is the combustion time scale. The last-named was originally equated to the turbulence dissipation time scale τ_t, defined as the ratio of the local turbulence energy k to its dissipation rate ε, i.e. $\tau_t = k/\varepsilon$. However this quantity falls toward zero as a wall is approached, leading to the unrealistic prediction that the burning rate tends to increase towards infinity. This in turn causes an increase in turbulent flame speed near the wall, a consequence of which is displayed in Fig.1. This shows the predicted flame evolution in a disc-chamber engine with a central spark location, calculated using an EBU model, with τ_c equated to τ_t, in combination with the k-ε model and associated wall functions. It is clear that the flame shape is incorrect, being inwards rather than outwards-curved: this is due to the burning-rate behaviour described above. In fact this example does not reveal the full extent of the problem, for if a low Reynolds number turbulence model is employed, the flame acceleration within the boundary layer may become very large indeed (7).

Also evident in Fig 1 is the excessive thickness of the flame, which is a manifestation of another, less obvious, modelling deficiency, connected with the use of ensemble averaging in general and the ensemble average velocity as the convective velocity in eqn (1) in particular. This matter is discussed in (7).

Ad-hoc measures were later introduced into EBU modelling by some workers (eg 1,2) to avoid the near-wall acceleration by, for example, setting

$$\tau_c = \tau_t + \tau_l \qquad (3)$$

where τ_l is a laminar combustion time scale, typically taken as the ratio of the laminar flame thickness to its speed, δ_l/S_l. Although this has the desired qualitative effect in reducing the near-wall burning rate (but not the excessive flame thickness), it has no real theoretical basis.

Within the TWF framework the burning rate is typically evaluated from an expression like the following, taken from (4):

$$\tilde{w} = C\rho_u\, I_0\, S_l \tilde{c}(1-\tilde{c})/\, L_f \qquad (4)$$

where C is an empirical coefficient, I_0 is a stretch function and L_f is a characteristic wrinkling scale of the flame, assumed to be directly proportional to the turbulence time scale, thus:

$$L_f = S_l \tau_t \qquad (5)$$

It may readily be seen that when equations (4) and (5) are combined, the burning rate turns out to be inversely proportional to τ_t. In our experience this gives rise to the same unrealistic flame behaviour as EBU models, evidenced in Fig.1, even when the flame straining effects are modelled via I_0 according to the recommendations of (4).

New Combustion Model. We now present the new modelling approach developed by Weller (10,11), which is fundamentally different from those just described, in two key respects. Firstly, it takes into account in a more rigorous and extensive way (10) the fact that the flame represents an effective discontinuity separating burned and unburned regions, which renders inappropriate conventional averaging techniques which assume smooth spatial variations. This is done by use of conditional averaging on the burnt and unburnt gas, which has the advantage of separating out effects due to the presence of the interface from those within the continuum fluids on either side: for example, it clarifies where gradient transport assumptions are appropriate or otherwise. Secondly, it also performs a detailed analysis of the flame area evolution, which in addition to accounting for area generation by interaction with both the mean flow and a (given) spectrum of turbulent eddies (11), also allows for destruction due to flame propogation (including cusp formation) and transport by convection and diffusion.

The full model resulting from these considerations is large and complex, mainly because it includes conditional-average momentum and continuity equations for each region, which reflect the fact that there is a jump in velocity across the flame due to the density change. It is shown in (10) that a simpler ensemble-average formulation involving just one set of continuity and momentum equations can be recovered by making a plausible assumption about the relation between the jump velocity, the density ratio, the local flame area and other quantities. Within this framework, if the flame is characterised by the distribution of the local ensemble-average regress variable b = 1 - c, then the associated transport equation is

$$\frac{\partial \bar{\rho}\tilde{b}}{\partial t} + \nabla.\bar{\rho}\tilde{U}\tilde{b} - \nabla.(\bar{\rho}\,\tilde{D}_b\,\nabla\tilde{b}) =$$

$$-\,[\bar{\rho}\xi + (\bar{\rho}_u - \bar{\rho})\,\min(\xi, \xi_{eq})]\, S_l\, |\nabla\tilde{b}| \qquad (6)$$

where ξ is the local wrinkle factor, which is defined as the wrinkled flame surface area per unit projected area. This quantity, which is related to the flame area per unit volume, Σ, and the turbulent:laminar flame speed ratio by

$$\xi = \frac{\Sigma}{|\nabla\tilde{b}|} = \frac{S_t}{S_l} \qquad (7)$$

can be calculated from its own evolution equation

$$\frac{\partial \xi}{\partial t} + \bar{U}_S \cdot \nabla \xi - \nabla \cdot \bar{D}_l \nabla \xi = G\xi - R\xi^2 + \xi \hat{n} \nabla \bar{U}_t \cdot \hat{n} - \frac{1}{\xi} \hat{n} \bar{U}_S \cdot \hat{n} + (S_l (\xi^2 - 1) \bar{D}_l \nabla \xi) \frac{\nabla |\nabla \bar{b}|}{|\nabla \bar{b}|} \quad (8)$$

Here the terms $G\xi$ and $R\xi^2$ stand for the rate of generation of wrinkles by turbulence and the rate of removal by flame propogation: the quantities G and R can either be obtained from a separate spectral model (11) or from the following approximate, but adequate, relations derived therefrom: $G=0.28/\tau_\eta$ and $R=G/\xi_{eq}$, where τ_η is the Kolmogorov time scale and ξ_{eq} is defined below.

Further and finally, the above 'two-equation' model can be reduced to a one-equation version by the assumption that local equilibrium between wrinkle generation and removal prevails, i.e. $\xi = \xi_{eq}$, in which case eqn (8) can be dispensed with and the rhs of eqn (6), which represents the mean reaction rate $\tilde{w}$ becomes:

$$\tilde{w} = \bar{\rho}_u \xi_{eq} S_l |\nabla \tilde{b}| \quad (9)$$

There are several noteworthy points about the above burning rate expression. It differs significantly in form from its EBU and TWF counterparts, eqns (2) and (4) respectively: in particular, it contains the product $\xi_{eq}|\nabla \tilde{b}|$, which from eqn (7) is seen to be the flame area per unit volume, which according to the present analysis is *not* simply related to the turbulence scales, as supposed by the earlier models. Of course ξ_{eq}, which it will be recalled is equal to the turbulent:laminar flame speed ratio, is itself an unknown, so additional information is required (it should be noted that this is not the case with the full two-equation version). This might be viewed as an advantage: indeed this model is unique in allowing the user to impose, via a burning rate function, any chosen turbulent flame speed behaviour, whether theoretically or empirically based.

In the present work the one-equation version of the new model is used, with both aforementioned kinds of flame speed input. Specifically, on the theoretical front we have used the spectral flame model of Weller et al (11) to generate predictions of S_t/S_l for flames initiated as a small laminar kernel in a homogeneous turbulence field. (The simulations, it should be noted, start after the period of strong thermal input from the spark processes (12), which is of about 300 μs duration and produces an initial laminar kernel of around 1.5 mm radius.) Fig 2 shows by way of example the predicted transient development for various levels of turbulence intensity u', and fixed values of turbulence length scale, laminar flame speed and its stretch/curvature response (obtained from laminar flamelet data), expansion ratio and other relevant parameters. The flame speed steadily rises from its laminar value as consequence of wrinkling by turbulence over an increasing range of scales, although there is a counter-effect due to stretch, especially when the kernel is small. Eventually a fully-developed state is reached, albeit not within the range of the plot, at which the flame is influenced by all scales. Fig 3 shows how the predicted fully-developed flame speed varies with turbulence intensity and the stretch extinction coefficient σ_{ext} with all other parameters held constant. Evidently when u'/S_l is less than about 4 the flame speed steadily increases with u' and is insensitive to stretch effects, but at higher values the latter become important and the rise is gradually arrested, followed by a decay. Results of this kind, which are in line with experimental findings(11), have been generated as input for the engine calculations with the one-equation model, as described in the next section.

As an alternative, the following semi-empirical correlation for the speed of a developing flame proposed by two of the present authors (13) has also been used

$$\frac{S_t}{S_l} = 1 + \left[\frac{u'}{u'+S_l}\right]^{1/2} \cdot \left[1 - e^{-\frac{S_l}{u'+S_l}\frac{t}{\tau}}\right]^{1/2} \cdot \left[1 - e^{-\frac{t}{\tau}}\right]^{1/2} \left(\frac{u'}{S_l}\right)^{5/6} \quad (10)$$

Here τ is a characteristic time scale, of recommended value 1.5 ms ms. This formula produces the same general trends evidenced in Figs 2 and 3.

Here τ is a characteristic time scale, of recommended value 1.5 ms.This formula produces the same general trends evidenced in Figs 2 and 3.

COMPARISON WITH EXPERIMENT

Description of Experiment. For the purposes of evaluating the combustion model and other aspects of the in-cylinder predictions, including the flow behaviour and charge/residual mixing, experiments were performed in a special optically-accessible square-piston engine (Fig 4). Details of its construction were provided in a previous COMODIA paper (14), so only a brief outline will be given here. The engine has a 'bore' of 75mm, stroke of 67mm and nominal compression ratio of 10.2. Optical access is available through all sides of the cylinder and a window in the two-valve cylinder head, which has a (nearly) central spark plug.

For the present experiments the engine was fueled with propane and skip-fired. Measurements were made of the spatial and temporal variations of the following quantities: (i) velocity in the valve curtain, by LDA at a limited number of points, for use as boundary conditions for the calculations; (ii) mixing and distribution of fuel concentration in selected planes during induction and compression, by planar laser-induced fluorescence (PLIF); (iii) evolution of the flame front in selected planes, by PLIF; (iv) instantaneous flow field in selected planes, by cycle-resolved particle image velocimetry (PIV). The data types (i) to (iii), along with the cylinder pressure, were gathered over at least 50 cycles, to produce the ensemble averages required for comparison with predictions.

Details of Calculations. The calculations were performed using the general-purpose STAR-CD code (15) which solves the governing equations, including those of the combustion model and the k-ε turbulence model, on an unstructured, moving mesh (Fig 5) here comprising about 40000 cells, facilitating proper representation of the (time-varying) geometry and resolution of the flow features. Economy and accuracy are further enhanced through the use of a time-implicit solution algorithm, with a time step of 0.15 CAD in conjunction with self-filtered second-order spatial differencing. The inputs to the simulation of the induction, compression and power strokes comprise the piston and valve motions, intake manifold and residual charge conditions, valve curtain velocities and spark timing.

Results and Discussion. We present here, for reasons of space limitations, extracts for a single operating point, corresponding to a speed of 1000 rpm, equivalence ratio 1.0, half load and ignition at 20 CAD BTDC. Fig 6 compares the measured and predicted mixing during induction, in the form of the fuel concentration distributions in a vertical plane bisecting the cylinder between the two valves, at two crank angles. The pictures clearly portray how the entering annular jet of fresh charge mixes with the residual gases. The agreement is reasonable, especially in view of the limited valve curtain flow data. At later stages closer to the time of ignition the calculations and experiments both indicate that the mixture becomes essentially homogeneous.

Fig 7 shows, in a parallel plane containing the intake valve axis, the calculated and measured flow patterns at 135 CAD BTDC. The measured data were obtained from an instantaneous PIV image and are therefore strictly not directly comparable, although low-pass filtering was used with a spatial resolution similar to the computational grid. The patterns are nevertheless similar in many respects, both qualitatively and quantitatively. Work is in progress to assemble ensemble-averaged images, to allow a more direct comparison.

Fig 8 displays the measured and predicted pressure histories for both motored and firing conditions. The close agreement with the motored curve was only obtained after incorporating and 'tuning' an orifice-type equation to model leakage past the piston rings, which was appreciable, due to the need to employ special rings and operate without oil to help keep the windows clean. This same leakage treatment, with unaltered coefficients, was used for the firing case, with the rather encouraging result shown in the same figure. Essentially identical predictions were obtained using either eqn (10) for the flame speed input or the results from the spectral simulations.

Of even greater encouragement are the comparisons in Fig 9 between the predicted and measured flame images in the same viewing plane as before, plotted in terms of progress variable: as expected the flames are thick, because they are ensemble averages. The first point to note is the correct qualitative behaviour of the predictions, as compared with Fig 1: evidently here the flame has the right sense of curvature and more reasonable thickness. The quantitative agreement is also fairly satisfactory. The flame thickness is somewhat greater than measured, but this is an expected consequence of the approximations invoked in going from the two-equation model to the one-equation version used here: the former would give a thinner flame. The predicted propagation rate is about right, which is consistent with the level of agreement obtained for the pressure history. At a more detailed level, at the very early stage the measured flame has an elliptical shape, while the predicted one is more spherical. There are many possible explanations for this, but the most likely causes are (a) an observed statistical lateral variation in the spark location of about ±1.5 mm; (b) the flame holder effect (12) producing an elongated spark channel due to the mean flow across the spark gap, and (c) a higher initial spark-assisted flame speed. All of these effects can, in principle, be incorporated into the present model.

CONCLUSIONS

We have described a combined computational and experimental study of homogeneous-charge engine combustion, in which CFD calculations employing a novel, fundamentally-based combustion model are compared with detailed experimental data gathered using advanced laser diagnostics in a special optical research engine. All the results are generally encouraging, but of particular significance is the close correspondence between the measured and predicted flame structures, which the new model produced without the need for ad-hoc measures. It is now necessary to extend the assessment over a wider range of data and operating conditions. This work is currently in progress.

REFERENCES

1. Abraham J, Bracco F V and Reitz R D "Comparisons of computer and measured premixed charge engine combustion" Combustion and Flame, 60:309-322, 1985.
2. Jennings M J "Multidimensional modelling of turbulent premixed charge combustion" SAE 920589, 1992.
3. Kuo Tang-Wei and Reitz R D "Computation of premixed-charge combustion in pancake and pent-roof engines" SAE 890670, 1989.
4. Bray K N C "Studies of the turbulent burning velcocity" Proc Royal Soc, London, A431, 1990.
5. El Tahry S H "A turbulent combustion model for premixed charge engines" GM Research Report FM-133, USA 1988.
6. Borghi R, Argueyrolles B, Gauffie S and Souhaite P "Application of a "Presumed pdf" model of turbulent combustion to reciprocating engines" 21st Symposium on Combustion, 1591-1599, The Combustion Institute, 1986.
7. Boudier P, Henriot S, Poinsot T and Baritaud T "A model for turbulent flame ingition and propagation in spark ignition engines" 24th Symposium on Combustion, 1992.
8. Torres A and Henriot S "3D modelling of combustion in lean-burn four-valve engines: influence of intake configuration" COMODIA'94.
9. Cheng W K and Diringer J A, SAE 910268, 1991
10. Weller H G "The development of a new flame area combustion model using conditional averaging" TF/9307, Mech Eng Dept, Imperial College, 1993.
11. Weller H G, Marooney C J and Gosman A D "A new spectral method for calculation of the time-varying varrea of a laminar flame in homogeneous turbulence"

23rd Symposium on Combustion, 629-636. The Combustion Institute, 1990.
12. Herweg R "Die entflammung brennbarer, turbulenter gemische durch electrische zündanlagen - bildung von flammenkernen" PhD Thesis, University of Stuttgart, 1992.
13. Maly R R and Herweg R "A fundamental model for flame kernel formation in SI engines" SAE 922243, 1992
14. Maly R R, Eberspach G and W Pfister "Laser Diagnostics for single cycle analysis of crank angle resolved length and time scales in engine combustion" Proc COMODIA'90, 399-404, JSME 1990.
15. Introduction to STAR-CD code. Computational Dynamics Limited, 1994.

ACKNOWLEDGEMENTS

This work was supported by Daimler Benz and the Commission of the European Communities.

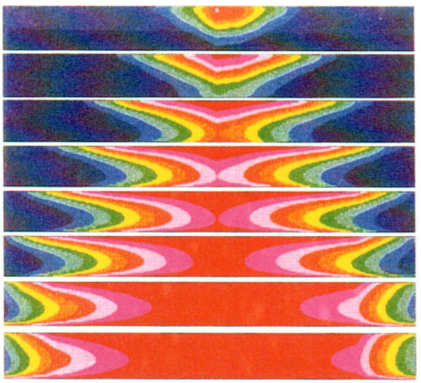

Fig 1 Flame evolution in disc-chamber engine as predicted by the standard EBU model, using $\tau_t = \tau_l$

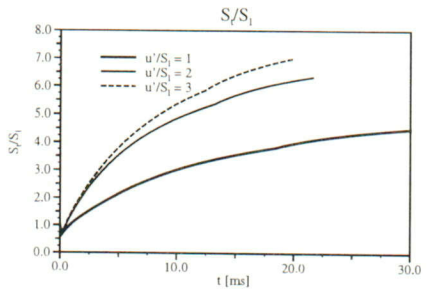

Fig 2 Spectral model prediction of transient turbulent flame development, starting from a spherical laminar kernel

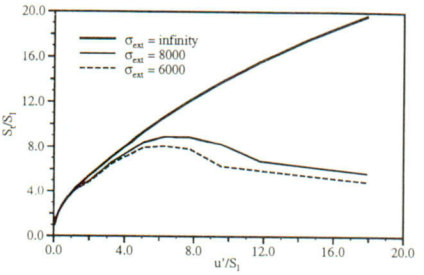

Fig 3 Spectral model prediction of fully-developed turbulent flame speed variation with turbulence intensity and stretch sensitivity

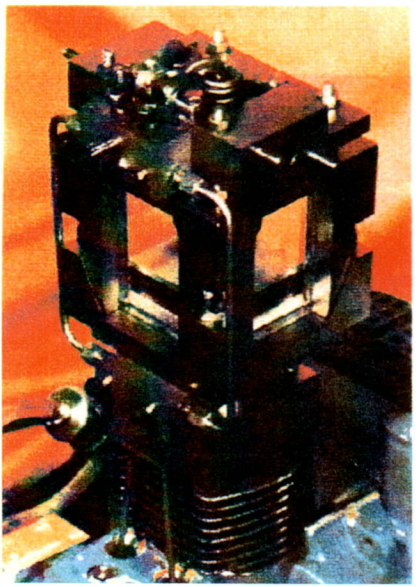

Fig 4 Daimler Benz optical square-piston research engine

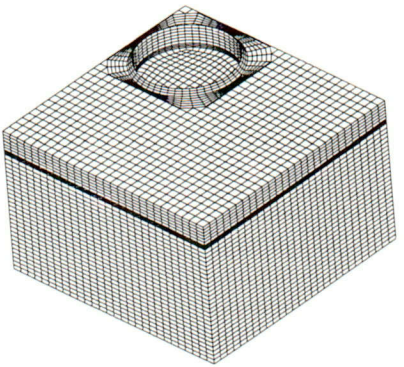

Fig 5 Computational grid structure at 90 CAD

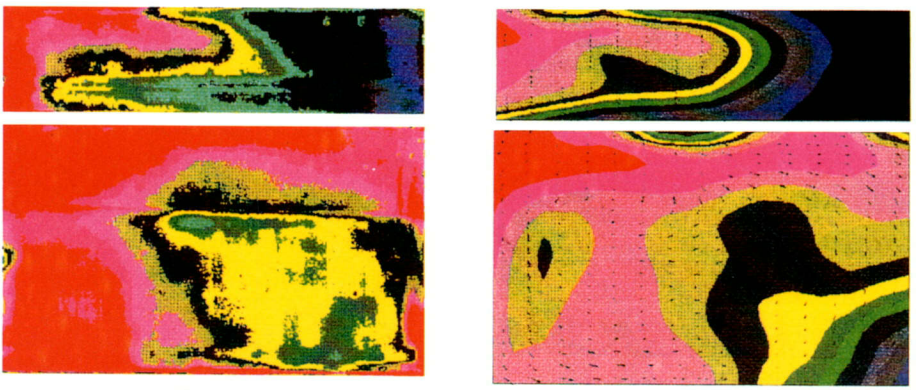

Fig 6 Measured (left) and predicted (right) ensemble-mean fuel distributions at (a) 45 CAD and (b) 90 CAD induction, in vertical plane between valves

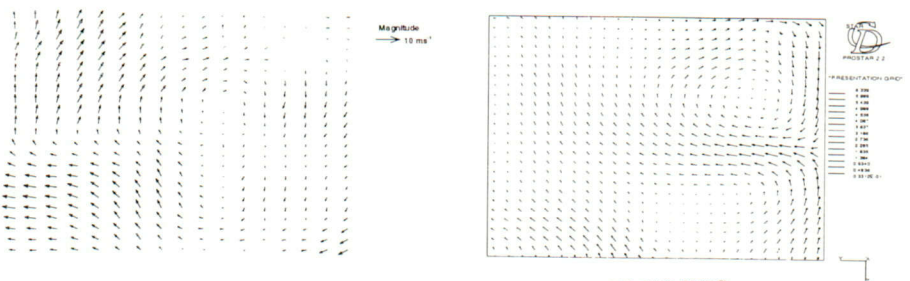

Fig 7 Measured (left) and predicted (right) flow fields at 135 CAD BTDC

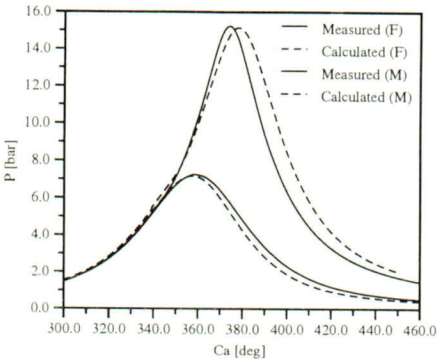

Fig 8 Measured and predicted cylinder pressure histories for motored (M) and and firing (F) conditions

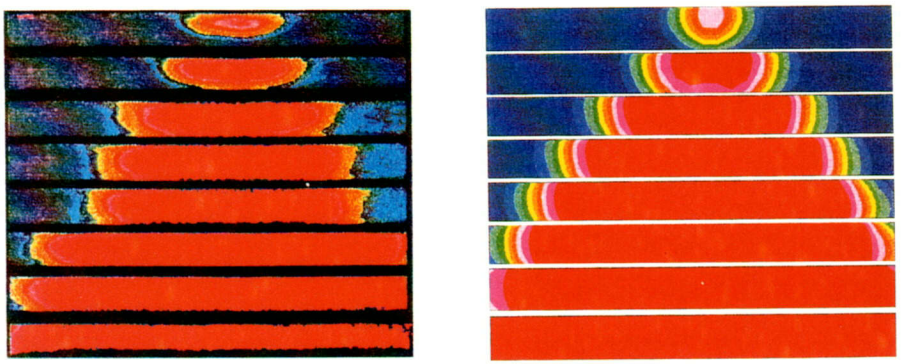

Fig 9 Measured (left) and predicted (right) ensemble-mean flame propagation (progress variable) in vertical plane between valves